1989

NASA/ASEE SUMMER FACULTY RESEARCH FELLOWSHIP PROGRAM

MARSHALL SPACE FLIGHT CENTER
UNIVERSITY OF ALABAMA IN HUNTSVILLE

A PARAMETRIC HEAT TRANSFER STUDY FOR CROGENIC BALL BEARINGS IN SSME HPOTP

Prepared by	Mingking K. Chyu
Academic Rank:	Assistant Professor
University and Department	Carnegie Mellon University Department. of Mechanical Engineering
NASA/MSFC:	
Laboratory:	Propulsion
Division:	Component Development
Branch:	Turbomachinery and Combustion Devices, EP62
MSFC Colleague:	James L. Cannon George M. Young, III
Date:	August 1989
Contract No.:	The University of Alabama in Huntsville NGT-01-008-021

A PARAMETRIC HEAT TRANSFER STUDY FOR CROGENIC BALL BEARINGS IN SSME HPOTP

Mingking.K. Chyu
Department of Mechanical Engineering
Carnegie Mellon University
Pittsburgh, PA 15213

James L. Cannon and George M. Young III
Propulsion Laboratory
NASA Marshall Space Flight Center
Huntsville, AL 35812

ABSTRACT

A numerical modeling is to examine the effects of coolant convective heat transfer coefficient and frictional heating on the local temperature characteristics of a ball element in SSME HPOTP bearing. The present modeling uses a control-volume based, finite-difference method to solve the non-dimensionalized heat conduction equation in spherical coordinate system. The dimensionless temperature is found as a function of Biot number, heat flux ratio between the two race contacts, and location in the ball. The current results show that, for a given cooling capability, the ball temperature generally increases almost linearly with the heat input from the race-contacts. This increase is always very high at one of the two contacts. An increase in heat transfer coefficient generally reduces the ball temperature and alleviates the temperature gradient, except for the regions very close to the race contacts. For a 10-fold increase of heat transfer coefficient, temperature decrease is 35% for the average over entire ball, and 10% at the inner-race contact. The corresponding change of temperature gradient displays opposing trends between the regions immediately adjacent to the contacts and the remaining portion of the ball. The average temperature gradient over the entire ball decreases about 50%. On the contrary, the temperature gradient in the vicinity of both contacts increases approximately 70% to 100%. A higher temperature gradient produces excessive thermal stress locally which may be detrimental to the material integrity. This, however, is the only unfavorable issue for an increase of heat transfer coefficient.

ACKNOWLEDGEMENTS

The first author (MKC) of this report is grateful to NASA-Marshall Space Flight Center and ASEE for the appointment of Summer Faculty Research Fellowship. In addition, he expresses special appreciation to Messrs. James L. Cannon and. George M. Young III for their collaboration in this project.

Thanks to Ms. Joan G. Trolinger for her help in collecting references, Mr. Craig Gilden for his assistance in preparing presentation material and Mr. Loren A. Gross for his enthusiastic interest in this project.

For Professor Gerald R. Karr and Dr. Frank Six, their excellent management of the entire program is highly appreciated.

LIST OF FIGURES

NOMENCLATURE

Bi	Biot number
h	heat transfer coefficient
k	thermal conductivity of bearing ball
Q_{ir} , Q.IR	ratio of heat flux at inner-race contact to that at outer-race contact
q_{or}, Q.OR	heat flux at outer-race contact
q	heat flux
R	dimensionless radial coordinate, see Equation (5)
r	radial coordinate
T	temperature
T.05	temperature corresponding to dimensionless temperature equal to 0.05
T.AVG	mean temperature averaged over entire ball
T.CENTER	temperature at ball center
T.INLET	temperature of LOx bulk temperature, -240 F in present study
T.IR	temperature at inner-race contact
T.OR	temperature at out-race contact
θ	azimuthal angle in spherical coordinate system, see Figure 3
ϕ	yaw angle in spherical coordinate system, see Figure 3
Θ	dimensionless temperature, see Equation (7)

Subscript

ir	contact of inner race
o	sphere outer surface
or	contact outer race
f	coolant fluid

INTRODUCTION AND RESEARCH OBJECTIVES

The reliability and service life of the ball bearings in the High-Pressure Oxidizer Turbo Pump (HPOTP) has become one of the most, if not the most, critical issues concerning the safety and future development of the Space Shuttle Main Engine (SSME). These bearings are operated under severe loading conditions with very high rotational speeds. Liquid Oxygen (LOx), the primary fluid media in HPOTP, is directed to flow through the bearings to provide cooling and lubrication. LOx with its cryogenic feature is an effective coolant but has poor lubrication capability. The present data has indicated that the actual bearing life is about one order of magnitude lower than that as designed for seven and one-half hours. This service-life is directly limited by fatigue and wear on the bearing components. Bearing removed from the pump has often shown discoloration which is evidently caused by intense surface oxidation and over-heating. The excessive heating is largely frictional and implies the current level of cooling and lubrication is apparently insufficient.

Significant endeavor on improving bearing service life and reliability has been pursued by NASA since early 1980's [1]. These include both testing and numerical modeling of the problem. At NASA Marshall Space Flight Center (MSFC), Bearing and Seal Material Tester (BSMT) was installed, with which near-engine, actual scale bearing testings can be performed. Data collected from BSMT provides basis for experimental investigation and modeling verification [2]. The modeling effort is primarily focused on the development of analytical tools for prediction of bearing behavior, in both mechanical and thermal aspects. There are two different approaches in present-day shuttle bearing modeling. One, using the SHABERTH/CINDA computer code, performs a lumped analysis with mechanical and thermal coupling [3]. The other employs computational fluid dynamics (CFD) which solves the transport equations numerically [4]. The CFD approach generally does not include mechanical modeling. Both approaches, to date, have shown success and continuing progress in certain areas; however, their potency to evolve as the ultimate design tool is still impervious. This is largely attributable to the lack of knowledge on coolant flow, bearing dynamics, ball-to-race interfacial friction and wear mechanism.

Despite these efforts, uncertainty still remains concerning the primary cause or causes for the bearing deterioration. It has been generally recognized for several years that the problem to the damage is primarily thermal. Under this notion, an improvement of the convective cooling can at least partially alleviate the problem. Thermodynamically, cryogenics are operated near the critical state, and the peculiarly-behaving properties under this condition often result in a higher heat transfer coefficient than those of subcritical states. The heat transfer coefficient can increase to an even higher value as a supercritical state is reached. Hydrodynamically, the nature of bearing flow is very complex as the axial through flow interacts with the rotational motions of balls and inner-race. Moreover, the combination of intense frictional heating and inadequate cooling may cause LOx vaporized in the vicinity of the ball surface. This boiling phenomenon further complicates the flow pattern and heat transfer to a great extent. The essential aspects of momentum and energy transport in the HPOTP bearings thus involve cryogenic, forced convection boiling in a rotating environment. A review of the literature reveals that virtually no study of this nature has been explored. The only relevant study has been done by Cuan et al. [5] who investigated

the effects of pressure and subcooling on the average heat transfer from a sphere with and without spinning in a pool of liquid-nitrogen. However, their data are still considered inadequate for actual bearing application.

Since the heat transfer information under the actual bearing environment is lacking, the pool boiling curve with a stationary sphere becomes the primary source of heat transfer data. Such a pool boiling curve for Oxygen is shown in Fig. 1. Note that the value of boiling heat transfer coefficient can differ by a factor of 10 or even 100 depending on the stage of boiling. Although it is a fact recognized widely that the ball surface is under the film boiling regime with low values of heat transfer coefficient, literally the entire spectrum of boiling can occur in different time, locations and loading conditions. Hence the choice of heat transfer coefficient of film boiling in a stationary pool as a valid representative for the bearing forced-flow is conservative and fundamentally incorrect.

The variation of heat transfer coefficient affects the temperature distribution in a bearing ball, which, in turn, influences the thermo-mechanical and wear properties of the material. To evaluate the nature of thermal expansion, thermal stress, and subsurface crack, the temperature distribution must be known as a priori. Thus it is necessary to gain detailed response of ball temperature to a change in the external heat transfer coefficient. The present study is primarily directed to fill this need. It uses a numerical method for a parametric analysis which covers a wide range of different cases. This includes the effect of different heating levels occurred at the contacts between the ball and two races.

Figure 2 shows the schematic sketch of a rolling ball and its adjacent races. Frictional heat is generated at the locations in contact with inner and outer races. For simplicity but without loss of generality, the ball is assumed rolling smoothly and with a very high speed; thus the two heated spots can be considered to be two heated "strips." The original three-dimensional problem can thus be reduced to a two-dimensional. Also shown in Fig. 2 are the locations and sizes of contact area. Measure of a contact area is given by the angle of opening, and it is assumed 8 degree for the outer-race and 5 degree for the inner race. The choice of these sizes are based on the corresponding magnitudes used in a recent CFD modeling by Owens [4]. In addition, any influence due to the presence of cage is assumed to be negligible. The following discusses the numerical computation which gives the details of the present analysis.

NUMERICAL COMPUTATION

The heat transfer in a ball element is governed by the following equation in spherical coordinate system as shown in Fig. 3.

$$\nabla \cdot (k \nabla T) = 0 \qquad (1)$$

where k is the thermal conductivity of the ball and $T = T(r, \theta, \phi)$ represents the temperature field. In the present analysis, k is assumed constant and Eq. (1) becomes a Laplace equation; i.e.,

$$\nabla^2 T = 0 \tag{2}$$

Furthermore, with the assumption of "strip heating" as mentioned earlier, the temperature dependency on ϕ.can be eliminated. Thus T is a function of r and θ.

The boundary conditions on the ball surface ($r = r_o$) are specified as

(i) At contacting area:

$$-k\,(\partial T/\partial r) = q \tag{3}$$

where q is the frictional heat flux generated on the contact area. Note that the value of q is different between contact with the inner-race (q_{ir}) and that with the outer-race (q_{or}).

(ii) At non-contacting area:

$$-k\,(\partial T/\partial r) = h\,(T - T_f) \tag{4}$$

where h is the convective heat transfer coefficient and T_f is the bulk temperature of the coolant flow.

To further extend the generality of the present analysis, the aforementioned governing equation and boundary conditions, eqs. (2) to (4), are transformed to their dimensionless counterparts. This is accomplished by introducing the following dimensionless variables; i.e.,

$$R = r/r_o \tag{5}$$

$$Q_{ir} = q_{ir}/q_{or}, \tag{6}$$

$$\Theta = (T - T_f)/(q_{or} r_o/k) \tag{7}$$

and

$$Bi = h r_o/k \tag{8}$$

where Bi is the Biot number representing the ratio of thermal resistance inside the sphere to that outside the sphere. The governing equation in dimensionless form is

$$\nabla^2 \Theta = 0 \tag{9}$$

and the boundary condition becomes

$$\nabla\Theta = 1 \qquad \text{at outer-race contact}$$

$$= Q_{ir} \qquad \text{at inner-race contact}$$

$= - Bi \Theta$ at non-contacting area (10)

Thus the solution Θ, a dimensionless temperature, is a function of R, θ, Q_{ir} and Bi. It represents a generalized solution for any variation of ball size, operating temperature, and heat transfer coefficient. The value of Q_{ir} ranges from 1.2, 2, to 7.5, and Bi varies between two cases, 1 and 10. These values are calculated based on the practical information and material properties of actual HPOTP bearings.

Equations (9) and (10) are solved numerically using a control-volume based finite-difference method described in detail by Patankar [6]. Although the present study requires only two-dimensional and steady-state calculation, the computer program developed herein is capable of solving three-dimensional, transient heat conduction problems in generalized, body-fitted coordinate systems. Of particular feature in this computer code is the implementation of the so-called periodic boundary condition in the azimuthal, θ, direction. At the boundary, say $\theta = 0$ and 2π, the dependent variable, Θ, and its associated quantities are not explicitly specified at these two grids, but they must be correspondingly equal, since the two grids are, in fact, the same point. In other words, for a given radial coordinate, all variables repeat themselves with a period of 2π. One effective solution strategy in dealing with problems with such a periodic nature is given by Patankar et al. [7], and it is adopted for the present computation. Here, the so-called Cyclic Tri-Diagonal Matrix Algorithm (CTDMA), facilitates a direct solution along the θ-coordinate. Correspondingly, in the radial direction where periodicity is non-existent, the non-cyclic version of such a direct solver, TDMA, is used. During a computation, the two direct solutions are swept across the entire domain in an alternate fashion using the so-called "line-by-line iteration." The iteration as well as the entire calculation procedure terminates at an attainment of a converged solution.

All the computations are performed with a grid of 40 and 100 points in R and θ direction, respectively. The choice of this grid size which gives sufficiently accurate data and reasonable computing time is a result of an extensive grid-independence study. The grid is nonuniform and denser near the outer surface and contact regions where steeper gradients of dependent variables exist. The convergence criterion is that the percentage change of a variable at any grid should be within 0.1%. A typical run on a Micro VAX II computer takes approximately 500 iterative steps with a CPU time about 1 minute. Note that the present numerical scheme, particularly for computing time, may not be the most efficient for solving heat conduction or diffusion dominant problems. However, the framework of the present program is designed to be completely compatible with one of the most effective, pressure-based computational fluid dynamics (CFD) code. Future extension in simultaneous modeling the heat convection in coolant flow and heat conduction in solid ball - a conjugate problem - is possible .

RESULTS AND DISCUSSION

The computed results are shown in figures 4 to 9, each of which includes a contour plot of the dimensionless temperature, Θ, and a table listing values of actual temperature and heat flux at locations of interest. The temperature and heat flux

shown in the table use the units of degree F and BTU per square foot per second, respectively. The actual temperature at any location, according to Eq. (7), can be inferred from the calculated Θ with given q_{or} and T_f. The value of T_f (denoted as T.INLET in tables) is taken at -240 degree F for all cases, which is the critical temperature of Oxygen. To facilitate the sample calculation, it uses five levels of q_{or} ranging from 100 to 1500 BTU/ft^2 sec as listed in the first column. The nomenclature stated in second row of the table, T.OR, T.IR, T.AVG and T.CENTER represent the temperature at outer-race contact, at inner-race contact, average over entire ball and at center, respectively. Note that T.05 stands for the actual temperature for $\Theta = 0.05$, and its values tabulated in the last column are correspondingly equal for all figures. This is rather obvious, since the relation between Θ and T is governed by Eq. (7) alone and independent of Bi and Q_{ir}, the primary variables between any two figures. The third row in these tables displays the numerical data of Θ for the corresponding temperature indicated in the second row.

For given values of Bi and Q_{ir} temperature in a sphere increases nearly linearly with the amount of frictional heating at the outer-race contact, q_{or}. This is clearly shown in the listed temperature of Figs. 4 to 9. Moreover, Figs. 10 and 11 respectively exhibit additional graphic view of this effect for the case Bi = 10, Q_{ir} = 1.2 and Bi = 1, Q_{ir} = 7.5. The overall thermal scale for the former is the lowest (coolest) and the highest (hottest) for the latter. An examination of these two figures reveals that the rate of temperature increase vs. q_{or} varies with differences in location, external cooling (Bi), and level of frictional heating (Q_{ir}). It is clear that the temperature at one of the race-contact areas has the highest rate of increase, and temperature averaged over the entire volume or at the center has the lowest increasing rate. For Q_{ir} = 1.2, representing an almost equivalent heat generation between the two race-contacts, the highest temperature as well as the increasing rate exists at the outer-race contact. However, for Q_{ir} = 7.5, such an extreme instead occurs at the inner-race contact. The value of Q_{ir} greater than unity implies that the heat flux at the inner-race contact is higher than that at the outer-race contact. Accordingly, the total heat generated and local temperature near the inner-race contact should be higher provided that both contact areas are of the same size. This is not the case for Q_{ir} = 1.2, because the area of outer-race contact is about 1.6 times higher than the inner-race contact. Thus the inner-race contact has a smaller amount of total heat generation and lower local temperature than its outer-race counterpart. For Q_{ir} = 2.0 or 7.5, the effect of area differential becomes secondary as the highly elevated heat flux dominates the local heating at the inner-race contact. As a result, the local temperature at the inner-race contact is higher than that of the outer race. For intense frictional heating, say $q_{or} \geq 500$ BTU/ft^2 sec, the temperature difference between the two contacts is nearly an order of magnitude for Bi = 1, Q_{ir} = 7.5, as Fig. 6 shows.

Of particular interest is to investigate the effects of external heat transfer coefficient on the ball temperature distribution. In the present dimensionless approach, this can be done by examining the variation of Θ as a function of Bi for a given Q_{ir}. According to the Θ definition (Eq. 7), such an effect is independent of the actual values of q_{or} and coolant temperature. Comparing the data shown in the third row of each table, as Bi increases from 1 to 10, the resulting decrease is approximately 35%, 8% and 10% for the temperature of average, outer-race contact and inner-race contact, respectively. To be noted is that these values are virtually independent of the relative

amount of heat generation between the two race-contacts (i.e., Q_{ir}), less than 1% within the present studying range. Apparently the temperatures at or near the contact areas is quite insensitive to the change of heat transfer coefficient. The rest of sphere reacts effectively and accordingly to the increase of heat transfer coefficient. Note that the temperature at the center core (fifth column in tables) is very close to the average temperature over the entire ball. This implies there are regions, mainly near the surface but away from the two contacts, the temperature reduction is more than 35%.

One general concern in cooling enhancement is the excessive temperature gradient accompanying with an overall temperature temperment. This is undesirable as additional thermal stress could result. An effective cooling scheme is capable of removing heat from the system by reducing its temperature uniformly throughout the entire domain. As observed in the contour plots for all cases, temperature gradients near a race contact is much greater than that of the remaining region, by nearly an order of magnitude. As expected, the lowest gradient typically occurs near the central portion of the sphere. The influence of Bi on the temperature gradient varies strongly with difference in location and level of contact heating.

An increase in Q_{ir} raises both temperature and temperature gradient in the vicinity of the inner-race contact. For a given Bi, the same effect, in fact, occurs in the remaining portion of the sphere, but to a much less extent. A comparison between Figs. 5 and 6 shows that, for Bi = 1 and Q_{ir} increasing from 2 to 7.5, the temperature gradient increases approximately 9 and 2.5 times at the inner-race contact and near the core region, respectively. This is understood as a stronger temperature gradient is established to facilitate the greater heat transfer for the case with a higher magnitude of Q_{ir}. Due to the absence of convective cooling at contacts, frictional heat in the present modeling must be transferred by conduction inside the ball first and then rejected from the surface by convection. However, the heat path is considered to be far more complex in actual bearing conditions. Heat transfer takes place in various mode among all the bearing constituents. Figure 12 displays a thermal coupling diagram to illustrate this phenomenon. In reality, the heat generation at a contact must be transferred with partitions among the ball, the race and the lubrication (coolant) film immediately adjacent to the contact. The last represents the only convection related effect and is little understood currently. The other two partitions are predominant by conduction, but the details of heat sharing can not be determined without considering the overall heat balance in the bearing system, as shown in Fig. 12.

For a given heating level at race contacts, one may expect that an increase in Bi or heat transfer coefficient will result in decreases of both temperature and temperature gradient. The former is true as discussed earlier; but the latter is not always the case. The fact is that, as Bi increases from 1 to 10, the temperature gradient decreases about 50% away from the contact zones, and, on the contrary, increases 70 to 100% in the close vicinity of both contacts. This is mainly caused by a much less temperature reduction at the contacts than in the remaining portion of the sphere, as the external cooling effectiveness increases. Such an elevation of temperature gradient near contact may be detrimental to the material integrity as the local thermal stress is expected to rise. However, this is the only unfavorable result due to the increase of heat transfer coefficient.

CONCLUSIONS

The effects of contact heating and heat transfer coefficient on the temperature in a HPOTP bearing ball is studied numerically. The present analysis solves the non-dimensionalized equation for heat conduction in a spherical domain. The boundary condition is comprised of two heated stripes, each representing the frictional heat generation at contact with one of the two races, and boiling convection of LOx on the remaining surface. For a given value of heat transfer coefficient, the ball temperature, in general, increases linearly with the heat input from the race-contacts. However, the actual trend of increase varies with location. The greatest increase occurs at one of the two contacts, the one that has the higher total heat generation.

An increase of heat transfer coefficient significantly decreases the ball temperature and alters its distribution. The present computation shows that, the average ball temperature decreases about 35% (with coolant bulk temperature as datum) for a 10-fold increment of the heat transfer coefficient. At the contacts, temperature decrease is much less, in the order of 10%, due mainly to the intense local heating. The corresponding change of temperature gradient is strongly dependent on the location, and opposite effects exist. For the major portion of the ball and away from the contact zones, the temperature gradient decreases about 50%. On the contrary, it increases 70 to 100% in the vicinity of both contacts. This increase of temperature gradient may cause the subsurface material become vulnerable and susceptible to wear. However, this is the only adverse effect induced by an increase in the heat transfer coefficient.

REFERENCES

1. Scibbe, H. and Dolan, F.J., "Bearing Technology - Overview," NASA CP 2372, *Advanced High Pressure O_2/H_2 Technology*, June, 1984, pp. 201-204.

2. Dolan, F.J., Gibson, H.G., Cannon, J.L. and Cody, J.C., "Cryogenic, High Speed, Turbopump Bearing Cooling Requirements," NASA CP 3012, *Advanced Earth-to-Orbit Propulsion Technology 1988*, pp. 110-132.

3. Cody, J.C., Marty, D.E. and Moore, J.D., "Evolution and Use of Combined Mechanical and Thermal Codes for Cryogenic Turbopump Bearings," NASA CP 3012, *Advanced Earth-to-Orbit Technology 1988*, pp. 88-101.

4. Owens, S.F., "Flow and Heat Transfer in the SSME HPOTP 4th Ball Bearing Assembly," CHAM 2005/5, February, 1989

5. Cuan, W.M. and Schwartz, S.H., "Pool Boiling From a Rotating and Stationary Spheres in Liquid Nitrogen," NASA CP 3012, *Advanced Earth-to-Orbit Propulsion Technology 1988*, pp. 142-158.

6. Patankar, S.V., *Numerical Heat Transfer and Fluid Flows*, McGraw-Hill, 1980

7. Patankar, S.V., Liu, C.H. and Sparrow, E.M., "The Periodic Thermally Developed Regime in Ducts with Streamwise Periodic Wall Temperature or Heat Flux," *J. Heat Transfer*, Vol. 99, 1977, pp. 180-186.

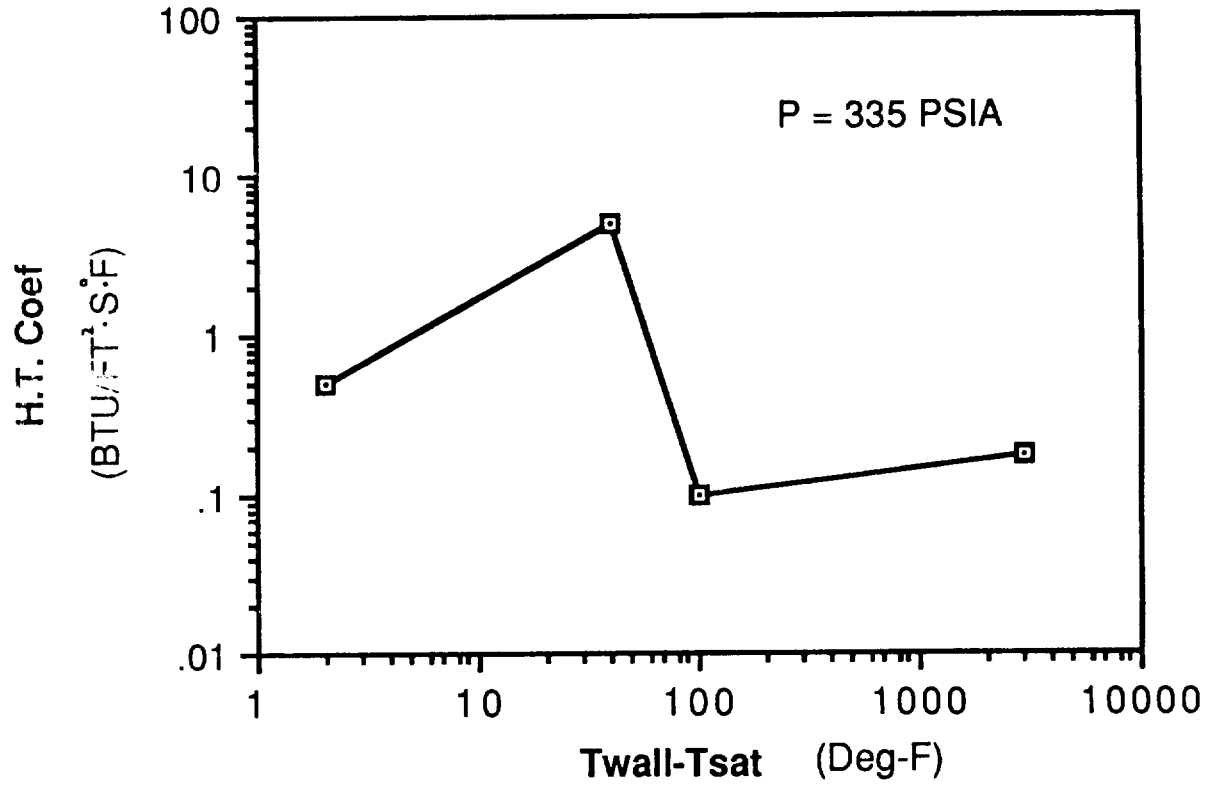

Figure 1. Heat Transfer Coefficient of Pool Boiling Oxygen

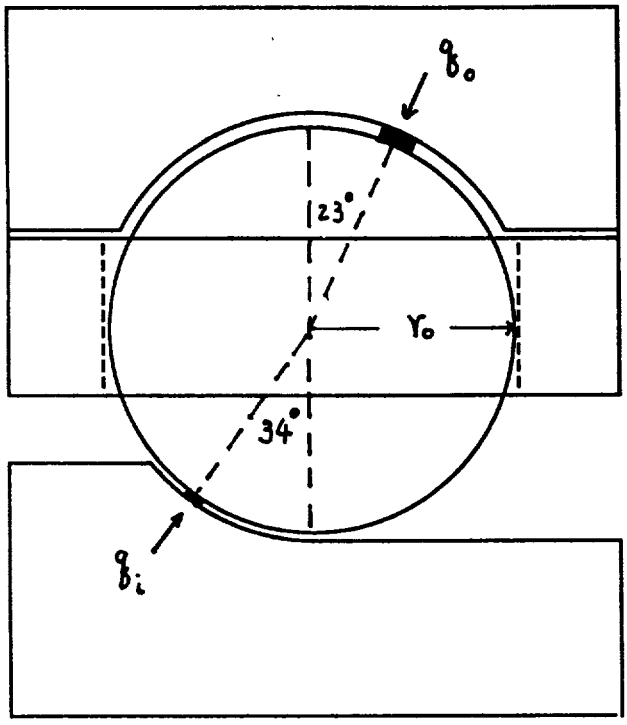

Figure 2. Rolling Ball Schematic

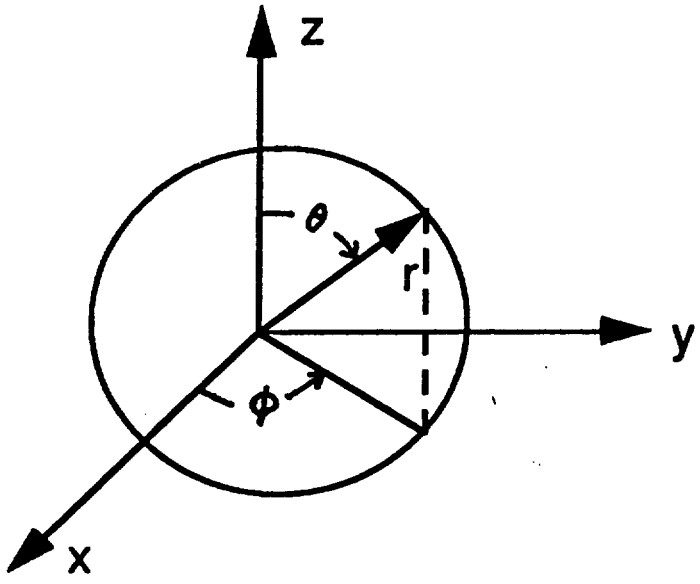

Figure 3. Spherical Coordinate System

Bi=1	Q.IR=1.2	DEG-F	T.INLET=-240		
QOR	T.OR	T.IR	T.AVG	T.CENTER	T.05
	0.114	0.109	0.026	0.025	0.05
100	-113	-119	-211	-212	-184
250	76.7	61.4	-168	-171	-101
500	393	363	-95.6	-102	37.8
1000	1027	966	48.8	36.7	316
1500	1660	1568	193	175	593

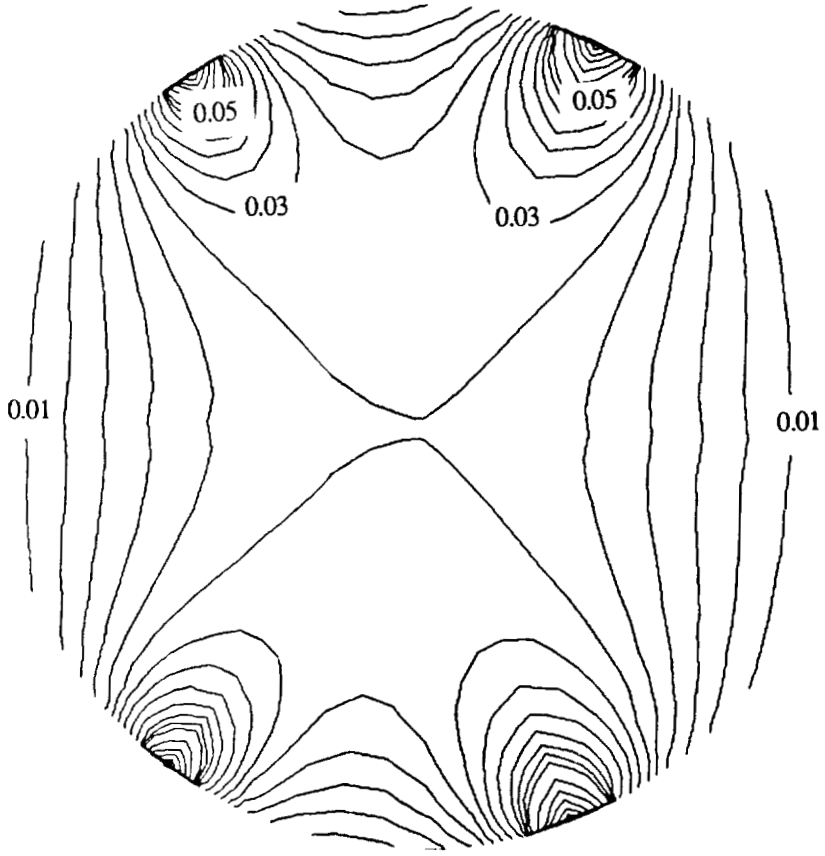

Figure 4. Ball Temperature Distribution, Bi = 1, Q_{ir} = 1.2

Bi=1	Q.IR=2	DEG-F	T.INLET=-240		
QOR	T.OR	T.IR	T.AVG	T.CENTER	T.05
	0.115	0.18	0.033	0.032	0.05
100	-112	-40	-203	-204	-184
250	79.5	260	-147	-151	-101
500	399	760	-51.4	-64.7	37.8
1000	1038	1760	131	117	316
1500	1677	2760	317	295	593

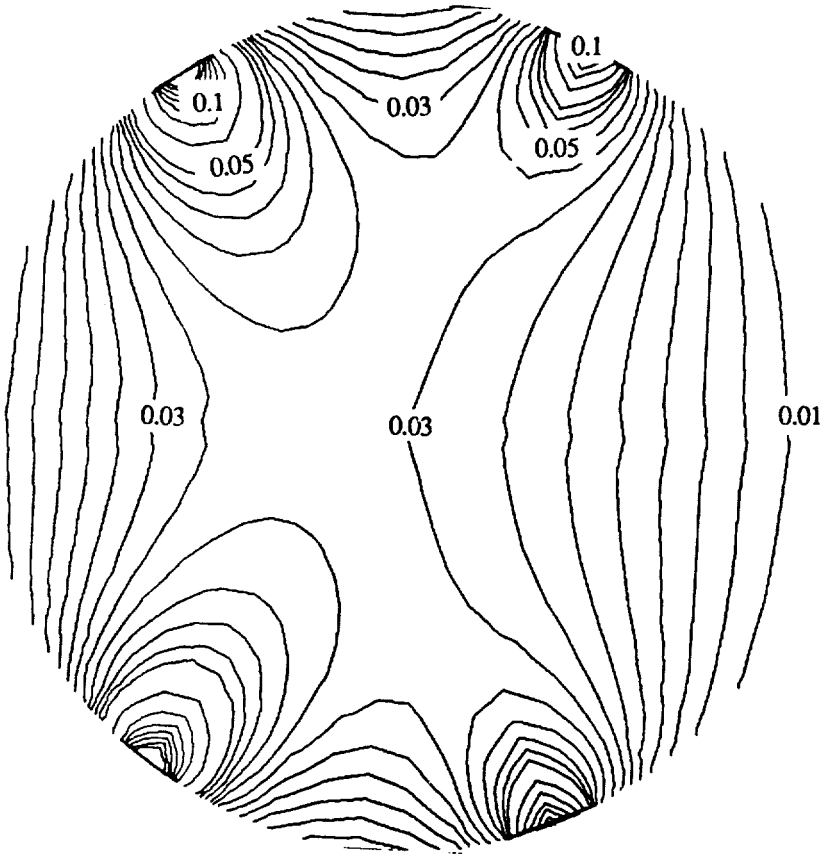

Figure 5. Ball Temperature Distribution, Bi = 1, Q_{ir} = 2.0

Bi=1	Q.IR=7.5	DEG-F	T.INLET=-240		
QOR	T.OR	T.IR	T.AVG	T.CENTER	T.05
	0.121	0.669	0.084	0.082	0.05
100	-105	504	-146	-149	-184
250	96.3	1619	-5.56	-13.6	-101
500	433	3478	229	213	37.8
1000	1106	7195	698	666	316
1500	1778	10913	1167	1118	593

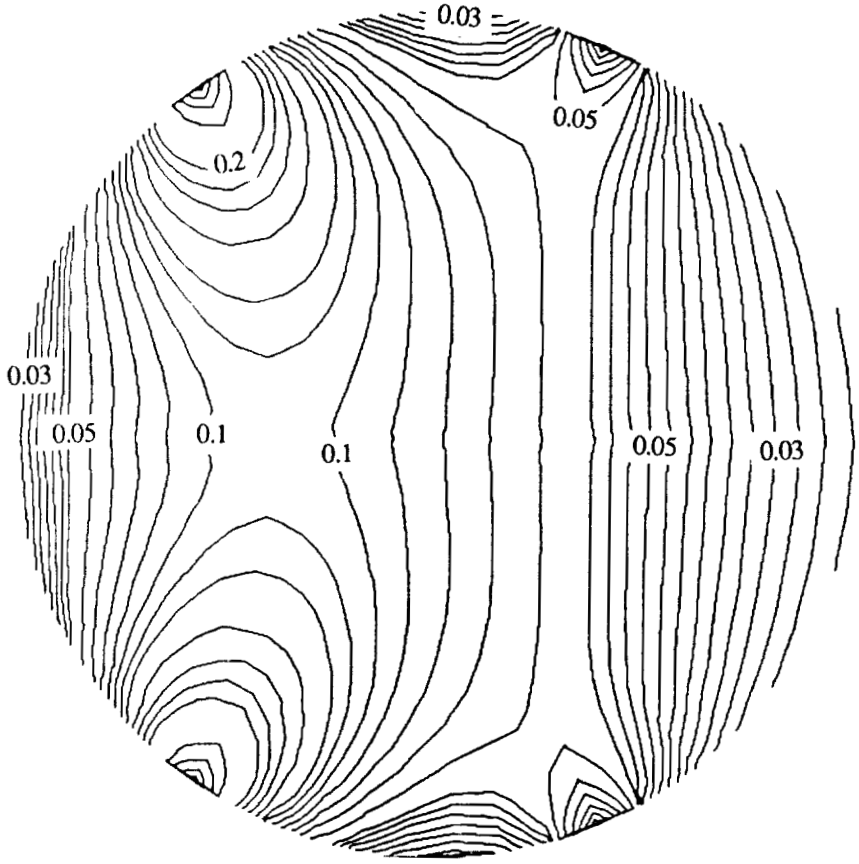

Figure 6. Ball Temperature Distribution, Bi = 1, Q_{ir} = 7.5

Bi=10	Q.IR=1.2	DEG-F	T.INLET=-240		
QOR	T.OR	T.IR	T.AVG	T.CENTER	T.05
	0.106	0.098	0.017	0.016	0.05
100	-122	-131	-221	-222	-184
250	54.5	31.7	-193	-194	-101
500	349	303	-146	-149	37.8
1000	938	847	-52.5	-58	316
1500	1527	1390	41.2	33	593

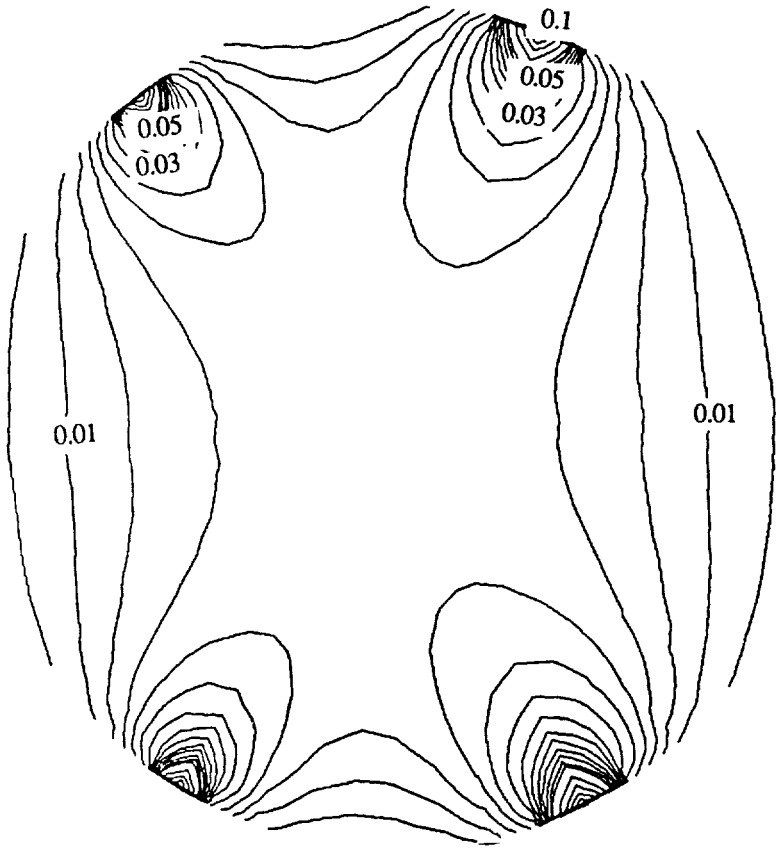

Figure 7. Ball Temperature Distribution, Bi = 10, Q_{ir} = 1.2

Bi=10	Q.IR=2	DEG-F	T.INLET=-240		
Q.OR	T.OR	T.IR	T.AVG	T.CENTER	T.05
	0.107	0.162	0.021	0.021	0.05
100	-122	-59.7	-216	-217	-184
250	56.1	211	-180	-182	-101
500	352	662	-121	-124	37.8
1000	945	1563	-1.76	-7.98	316
1500	1537	2465	117	108	593

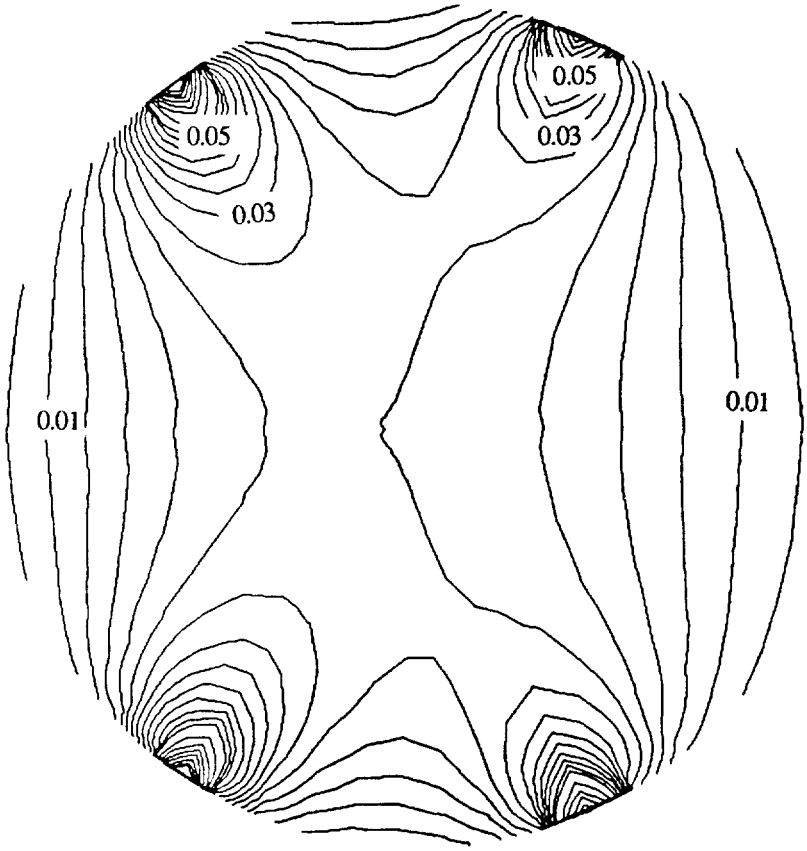

Figure 8. Ball Temperature Distribution, Bi = 10, Q_{ir} = 2.0

Bi=10	Q.IR=7.5	DEG-F	T.INLET=-240		
Q.OR	T.OR	T.IR	T.AVG	T.CENTER	T.05
	0.11	0.606	0.053	0.05	0.05
100	-117	433	-181	-182	-184
250	65.7	1443	-93.2	-96.1	-101
500	371	3126	53.6	47.9	37.8
1000	983	6492	347	336	316
1500	1594	9858	641	624	593

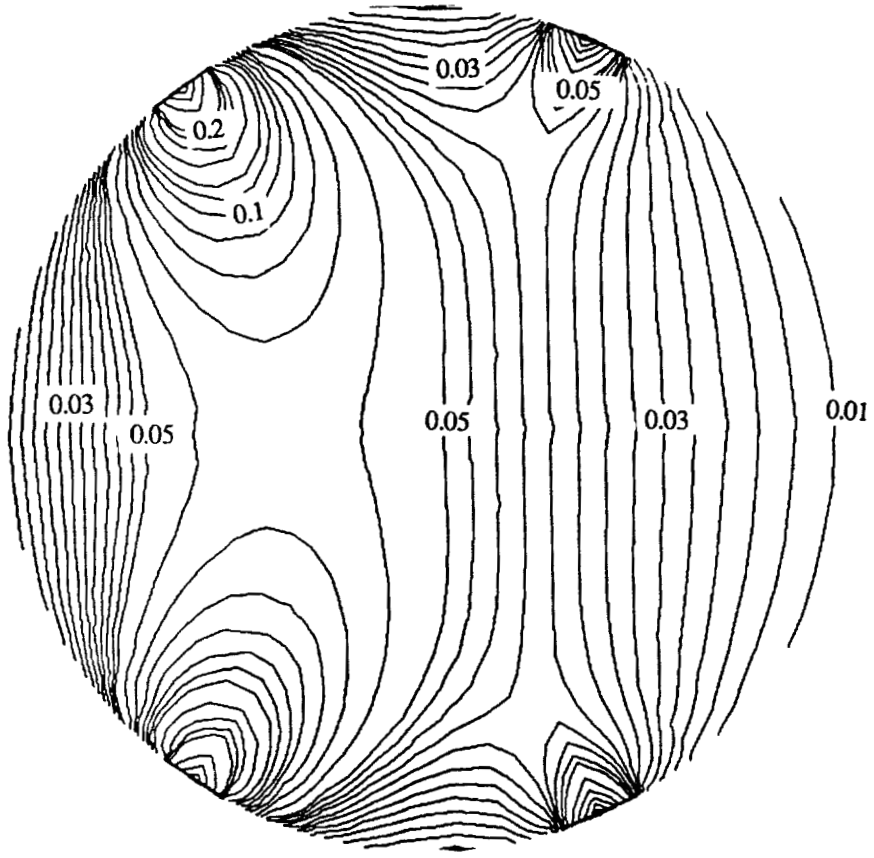

Figure 9. Ball Temperature Distribution, Bi = 10, Q_{ir} = 7.5

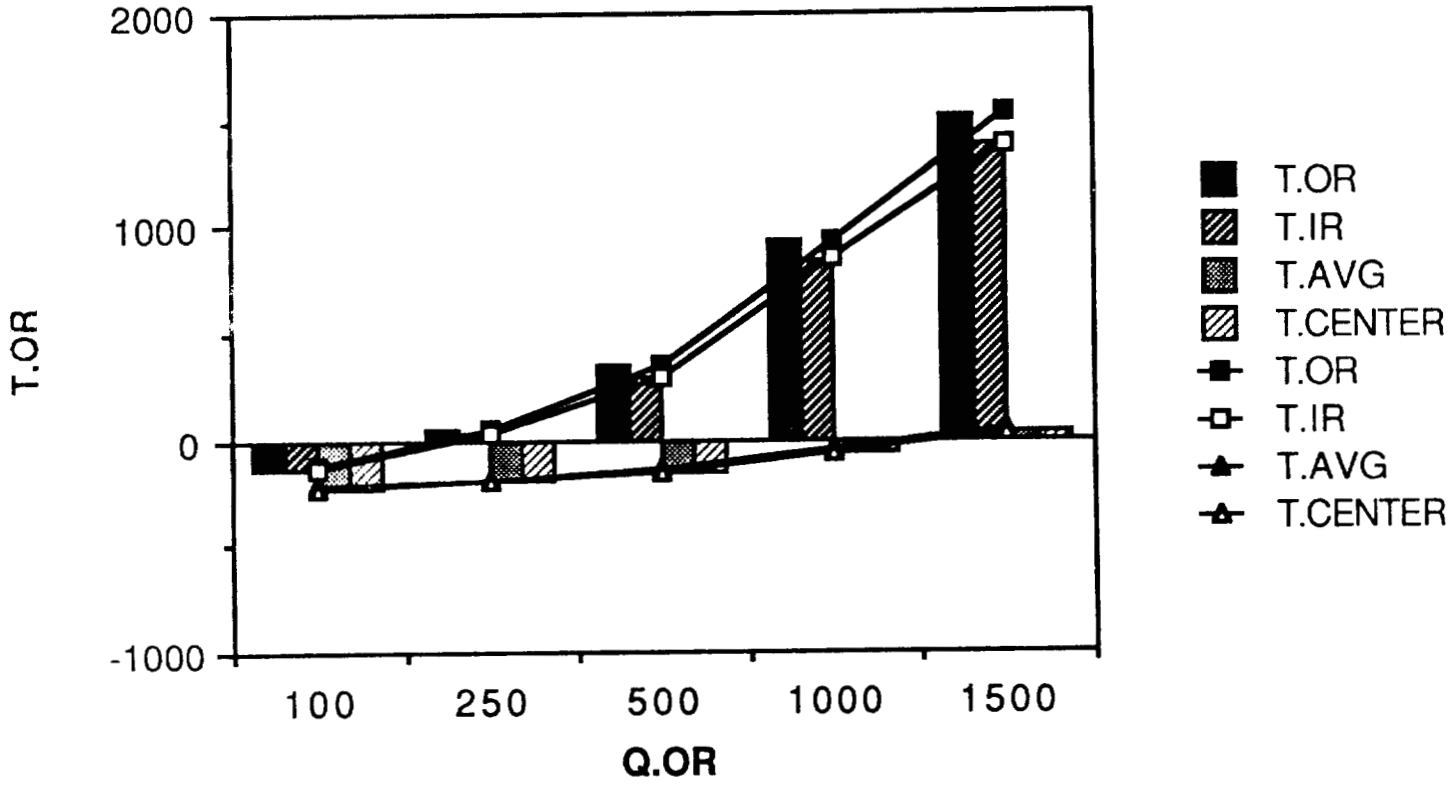

Figure 10 Effect of q_{or} on Ball Temperature Variation, Bi = 10, Q_{ir} = 1.2

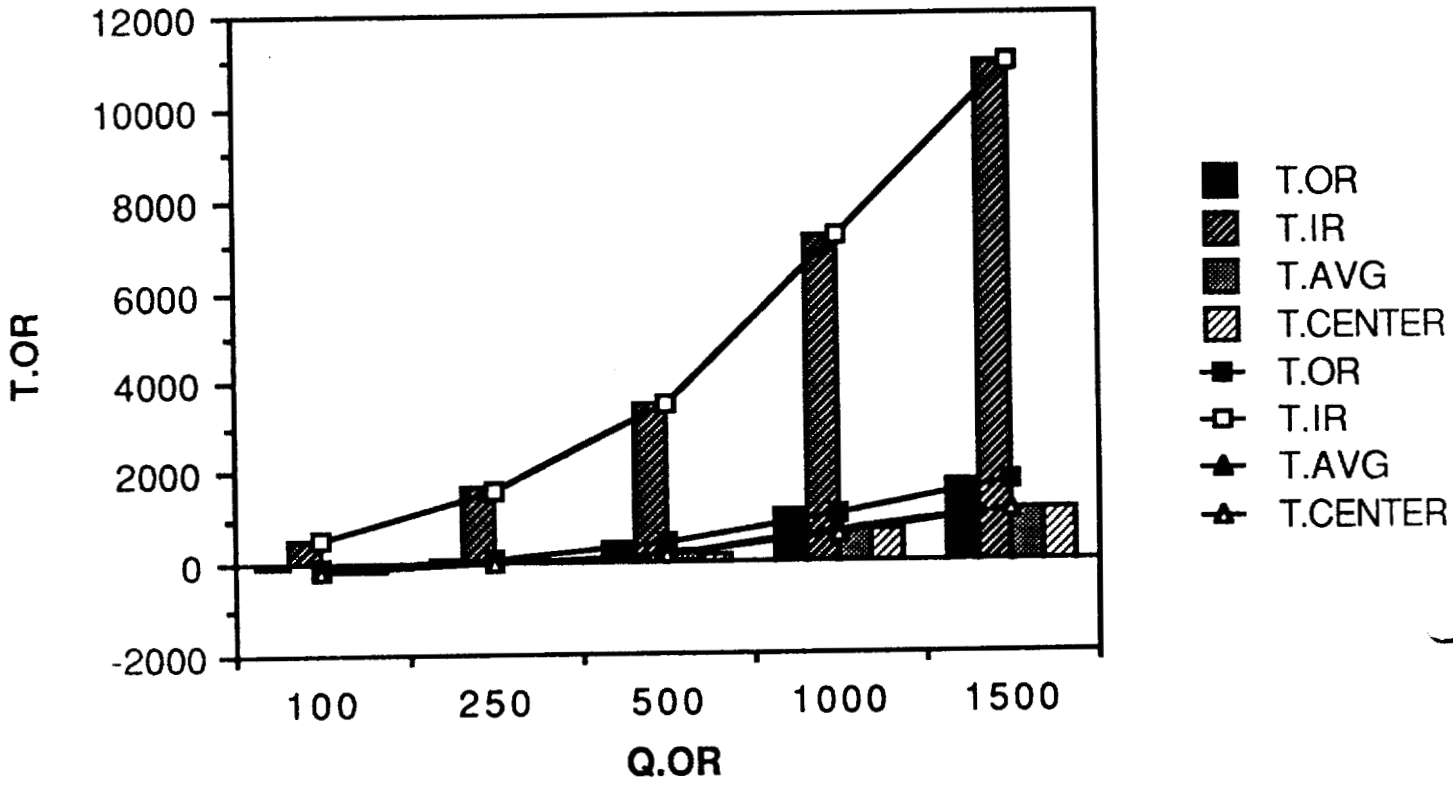

Figure 11 Effect of q_{or} on Ball Temperature Variation, Bi = 1, Q_{ir} = 7.5

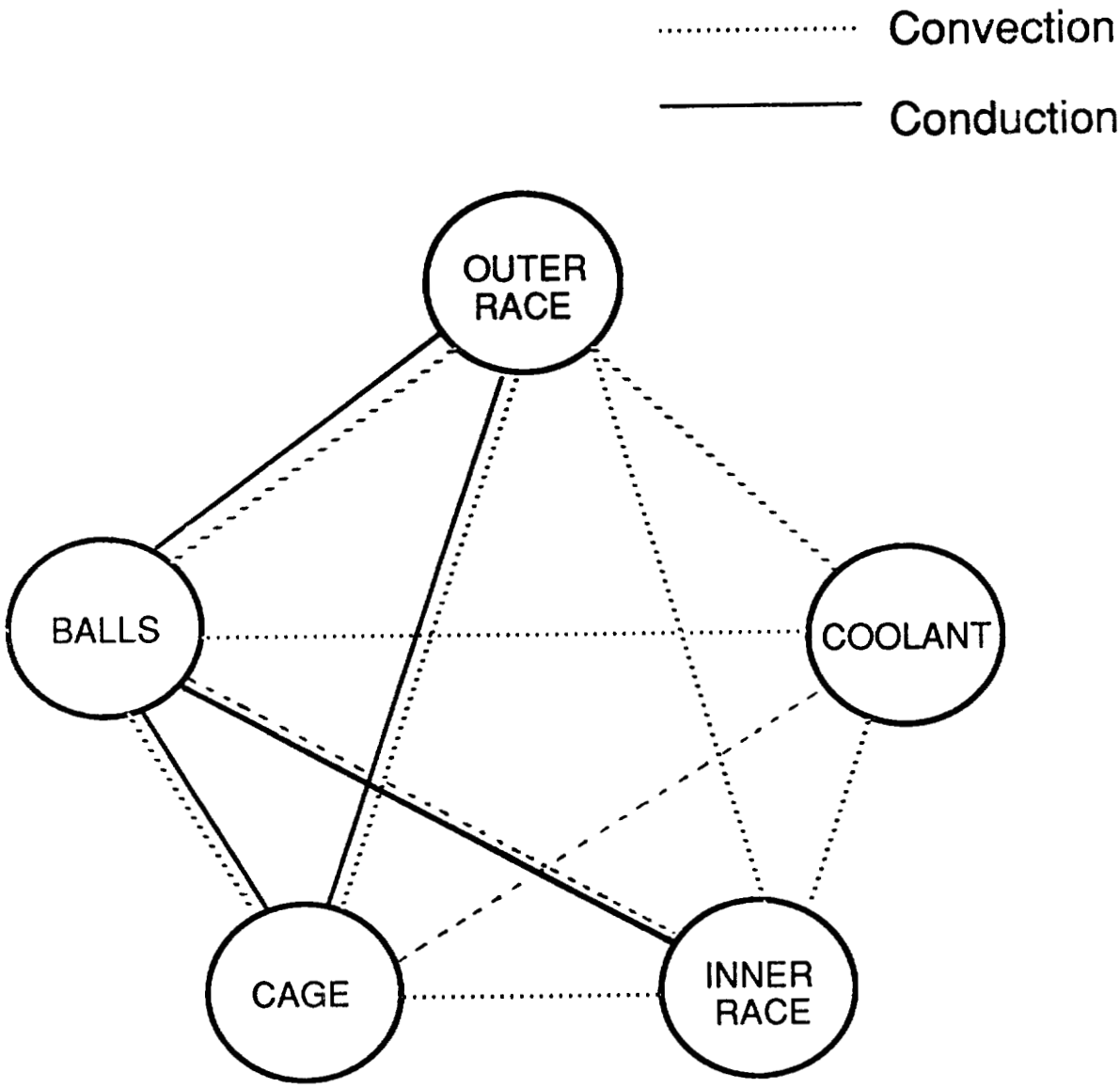

Figure 12. Thermal Coupling of Bearing Elements